

APPENDIX C

A list of parameters is presented here, for convenience.

C_{ii}^{elastic} is the usual elastic constant; $C_{ii}^{\text{magnetoelastic}}$ is the magnetoelastic contribution to the usual elastic constant; J_{ij} is the exchange integral; H_e is the effective magnetic field; H_0 is the applied magnetic field; ϵ_1^α , ϵ_2^α , ϵ_1^γ , ϵ_2^γ , ϵ_1^e , and ϵ_2^e are elastic strains written in hexagonal symmetry notation; B_{12}^α and B_{22}^α are axial single-ion magnetoelastic coupling constants; B^e is the shear single-ion magnetoelastic coupling constant; P_2 , P_4 , and P_6 are axial anisotropy coefficients; D_{11}^α , D_{12}^α , D_{21}^α , and D_{22}^α are axial

two-ion magnetoelastic coupling constants; λ_{kf} = λ_{11}^α , λ_{12}^α , λ_{21}^α , and λ_{22}^α are axial magnetoelastic coefficients; $\mathcal{L}_f(T, H)$ and $\mathcal{L}_{f\beta}(T, H)$ are longitudinal single-ion and two-ion spin correlation functions, respectively; $m(T, H)$ is the reduced magnetization; $\delta l/l$ is the linear dilation; $R_{i, i=0,1,\dots,5}$ are experimentally measured magnetoelastic constants; $I_{k+1/2}(x)$ are hyperbolic Bessel functions of half-odd integer power; θ is the magnetization angle measured from c axis; \bar{A} , \bar{B} , \bar{C} , \bar{D} , \bar{E} , and \bar{F} are coefficients of energy terms, defined in Eq. (34); $\beta_k = 1/k_B T$; μ_B is the Bohr magneton; and n_s is the number of nearest neighbors.

*Supported in part by the National Science Foundation and the Office of Naval Research, Contract No. N00014-69-A-0200-4032.

¹H. E. Nigh, S. Legvold, and F. H. Spedding, *Phys. Rev.* **132**, 1092 (1963).

²G. Will, R. Nathans, and H. A. Alperin, *J. Appl. Phys.* **35**, 1045 (1964).

³J. W. Cable and E. O. Wollan, *Phys. Rev.* **165**, 733 (1968).

⁴C. D. Graham, Jr., in *Proceedings of the International Conference on Magnetism, Nottingham, England*, 1964 (The Institute of Physics and The Physical Society, London, 1965).

⁵M. I. Darby and K. N. R. Taylor, *Ref. 4*, p. 742.

⁶D. S. Rodbell and T. W. Moore, *Ref. 4*, p. 427.

⁷W. D. Corner, W. C. Roe, and K. N. R. Taylor, *Proc. Phys. Soc. (London)* **80**, 927 (1962).

⁸J. Alstad and S. Legvold, *J. Appl. Phys.* **35**, 1752 (1964).

⁹R. M. Bozorth and T. Wakiyama, *J. Phys. Soc. Japan*

18, 97 (1963).

¹⁰W. E. Coleman, dissertation (West Virginia University, Morgantown, W. Va., 1964) (unpublished); E. Coleman and A. S. Pavlovic, *J. Phys. Chem. Solids* **26**, 691 (1965).

¹¹M. Long, Jr., U. C. L. A. Engineering Report No. 68-30, 1968 (unpublished); M. Long, Jr., A. R. Wazzan, and V. R. Stern, *Phys. Rev.* **178**, 775 (1969).

¹²E. S. Fisher and D. Dever, *Proceedings of Oak Ridge Conference on Rare Earths*, 1968, p. 522 (unpublished).

¹³H. B. Callen and E. Callen, *Phys. Rev.* **139**, A455 (1965).

¹⁴H. B. Callen and E. Callen, *J. Phys. Chem Solids* **27**, 1271 (1966).

¹⁵R. L. Melcher and D. I. Bolef, *Phys. Rev.* **178**, 864 (1969); **186**, 491 (1969).

¹⁶L. M. Levinson and S. Shtrikman, *J. Phys. Chem. Solids* **32**, 981 (1971).

¹⁷A. H. Morrish, *The Physical Principles of Magnetism* (Wiley, New York, 1965).

Low-Frequency de Haas-van Alphen Effect in Cobalt

I. Rosenman and F. Batallan

*Groupe de Physique des Solides de l'École Normale Supérieure,
Tour 23-9, quai Saint-Bernard-Paris 5e, France*

(Received 12 April 1971)

The Fermi surface (FS) of ferromagnetic cobalt has been investigated using the de Haas-van Alphen effect. Measurements were made at temperatures down to 1.1°K and magnetic fields up to 78 kOe using a low-frequency field-modulation technique. Since cobalt is ferromagnetic, the dHvA oscillations are periodic in B^{-1} rather than H^{-1} , as in nonmagnetic metals. Orientation studies of the dHvA frequencies in the (10 $\bar{1}$ 0) plane show two sets of frequencies. The lower set [(1-2) $\times 10^6$ G] has two branches and may be tentatively assigned to pockets of U symmetry of the spin-down FS. The higher frequencies [(3-5) $\times 10^6$ G], which can be observed up to 39° away from the hexad axis, were attributed to the existence of a neck at the Γ point of the spin-up FS. Agreement with band calculations is found if some modifications are made to the published FS models, mainly by reducing the exchange energy to fit the value found by photoemission studies. dHvA frequencies of (11-14) $\times 10^6$ G were also observed, but are still unexplained.

I. INTRODUCTION

The understanding of the ferromagnetism of tran-

sition metals on the basis of an itinerant-electron model¹ has made great progress in recent years— theoretically with band-structure calculations, as

well as experimentally. Among the experimental methods used, the most fruitful were photoemission for density-of-states determination and magnetoresistance and de Haas-van Alphen effect (dHvA) studies of the Fermi surface (FS).² The latter is very powerful in giving directly the extremal cross sections of the FS and the associated cyclotron masses.

We present here the results of our investigation of the FS of cobalt by the dHvA effect. Some very preliminary results have already been briefly presented.³

Cobalt is the only hcp ferromagnetic transition metal. Its very intricate band structure is insufficiently understood.⁴⁻⁶ The lack of experimental results makes its elaboration difficult, and does not make it possible to work out the interpolation schemes which were used successfully for other transition metals.⁷ Reed and Fawcett⁸ have shown by magnetoresistance studies some time ago that cobalt is an uncompensated metal. They have also observed, near the hexad axis, an oscillation in the magnetoresistance which they have attributed to magnetic breakdown. Eastman,⁹ from his recent investigation of the photoemission, has concluded that the exchange energy in cobalt is about 1.05 eV, a value which is in agreement with the value 1.05 ± 0.3 eV suggested by Wohlfarth.⁴

In Sec. II we will briefly describe our experimental method, stressing some modifications of the usual dHvA techniques imposed by the study of magnetic metals. Section III is devoted to the presentation of the experimental results concerning the determination of the internal magnetic field, the low dHvA frequencies α and β , and the cyclotron effective mass of β -orbit electrons. We summarize briefly in Sec. IV two published cobalt band-structure calculations^{5,6} which we use in Sec. V to discuss our results. We propose some modifications which may account for our observed dHvA results.

II. EXPERIMENTAL METHOD

Quantum oscillations of the electron-gas magnetic susceptibility vs magnetic field, known as the dHvA effect, are related to the structure of the FS. The oscillations are periodic in $1/B$, where B is the magnetic induction. The frequency is dependent on the cross-sectional area of the FS, through Onsager's relation

$$F(\theta, \phi) = \frac{\hbar}{2\pi e} \alpha(\theta, \phi), \quad (1)$$

where θ and ϕ are the polar coordinates of the magnetic induction with respect to the crystallographic axes of the sample. The amplitude A of the dHvA oscillations is given by the relation

$$A(B, T, \theta, \phi) = \frac{\lambda(B, \theta, \phi)T}{\sinh[2\pi^2 k T m^*(\theta, \phi) / \hbar e B]}, \quad (2)$$

where T is the temperature and $m^*(\theta, \phi)$ is the cyclotron effective mass.

We have used the low-frequency modulation of the magnetic field (LFFM) technique.^{10,11} The main magnetic field H is produced by a 78-kOe superconducting coil immersed in liquid helium at 4.2 °K. The sample is placed in a rotating sample holder inserted in an inner cryostat. The modulation field h , parallel to H , is produced by a coil made of superconducting multistrand copper stabilized wire for ac current. This coil is wound and fixed by epoxy on the tail of the inner cryostat in order to reduce the vibrations and produces a maximum modulation field h of 700 Oe. The frequency used is $\nu = 60$ cps.¹² The amplitude of h is either constant or programmably proportional to B^2 (Stark's overmodulation¹¹). Stark's overmodulation is used in order to keep z , the argument of the Bessel function found in the LFFM technique, constant:

$$z = 2\pi F h / B^2, \quad (3)$$

where

$$B = H + H_I, \quad (4)$$

$$H_I = 4\pi(1 - D)M_s. \quad (5)$$

B is the magnetic induction, H is the main external magnetic field, H_I is the internal magnetic field, D the geometrical demagnetizing factor, and M_s is the saturation magnetization. In a nonmagnetic metal one would simply have $B = H$ [instead of Eq. (4)]. (We have taken $\mu_0 = 1$.)

Detection of the dHvA effect was made by a system of two pickup coils wound around the sample, connected in opposition, and compensated in the absence of the sample. The internal coil had a rectangular cross section and was strongly electromagnetically coupled to the sample, whereas the external one, with circular cross section, was loosely coupled. Both coils were wound with $\frac{4}{100}$ -mm-diam copper wire using Ge 7031 varnish to glue them to the coil former and may rotate with the specimen in the sample holder.

The frequency ν in the pickup signal was rejected by a twin- T passive filter and the part of the signal either at 2 or 4ν was detected by a lock-in amplifier tuned to that frequency. The resulting voltage, if necessary fed through a very low-frequency filter, was recorded on an X - Y recorder and/or a digital printer so that the data could be processed by a computer.

The cobalt sample was spark-cut in a disc shape from an x-ray-oriented single crystal purchased from Ventron Electronic Corp., Bradford, Penn. After etching and heat treatment in a slightly oxidizing atmosphere (10^{-4} Torr oxygen), the specimen was annealed in vacuum (10^{-6} Torr). A control

sample from the same single crystal had a residual resistance ratio of about 220 after treatment. The sample was glued inside the inner pickup coil. The disc was rotated around its axis, which is perpendicular to H , so that the geometrical demagnetizing factor, and hence the internal field, remained constant. The axis was oriented along the $[10\bar{1}0]$ direction.

III. RESULTS

A. Internal Field H_I Determination

Since cobalt is ferromagnetic, the dHvA oscillations are periodic in $1/B = 1/(H + H_I)$ instead of $1/H$ as for a normal metal.¹³ First of all, one must determine H_I which, in our case, is constant. H_I is obtained in the following manner¹⁴: The magnetic-field values H_n corresponding to the dHvA-oscillation extrema are numbered with successive integers n . Since they are periodic in $1/B$, $1/B_n = 1/(H_n + H_I)$ must be a linear function of n when H_I has the correct value. For every value of H_I one computes the rms deviation Δ by least-squares fitting the $1/B_n$ vs n variation to a straight line. The value of H_I corresponding to the minimum Δ is chosen as the correct value of the internal field (Fig. 1).

The constancy of H_I ¹⁵ has been checked when the angle of \vec{H} relative to the \vec{c} axis varies in the range of 30° . The dispersion of the values around the mean value of 14 700 G is ± 500 G and because of the experimental errors is erratic. This uncertainty in H_I is an important cause of error in B determination and hence in the dHvA frequencies. We will take a value of $H_I = 14\,700$ G for all orientations of our specimen. When the disc shape of the sample is roughly approximated by an ellipsoid with the same axes, and the corresponding geometrical demagnetizing factor is used, we find $H_I = 14\,100$ G,

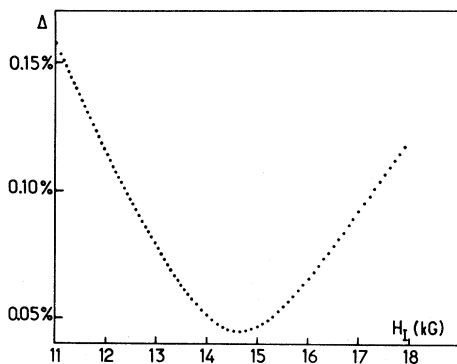


FIG. 1. Determination of the internal magnetic field $H_I = 4\pi(1-D)M_s$. rms deviation Δ vs H_I is plotted. A linear fit is made to $(H + H_I)^{-1}$ vs peak number n of the dHvA oscillation. H_I is treated as a parameter, and we choose the value which minimizes Δ . Here $H_I = 14\,700$ Oe.

in good agreement with the previous value.

B. dHvA Frequencies

In simple cases when there is a single or a dominant oscillation, the dHvA frequency is obtained either (i) from the X - Y recording in B , by using the formula $F = nB_1B_2/(B_1 - B_2)$, where n is the number of oscillations between two magnetic fields B_1 and B_2 , or (ii) from the $1/B$ recording, which, after calibration, gives the period directly and permits a check on the $1/B$ periodicity (Fig. 2).

In more intricate cases the numerical data were processed. The computer program makes a Fourier transform after correcting (linearly or parabolically) the nonoscillatory part of the susceptibility variation. Such an example is shown in Fig. 3. Figure 3(a) represents a recorder trace of dHvA oscillation at the highest magnetic fields and lowest temperatures (1.1°K) used. This curve was obtained for $\vec{B} \parallel \vec{c}$ axis with a sample in the shape of a cylinder elongated along the c axis, contrary to all other experiments. On this chart two kinds of frequencies are visible, one for the lower fields in the range $(11-13) \times 10^6$ G. The exact values may be drawn from the Fourier spectrum represented on Fig. 3(b), where the amplitudes are fitted vs frequencies. The following dHvA frequencies are visible: 3.7×10^6 G corresponding to β , 7.4×10^6 G which is the harmonic 2β , and a set γ , δ , and n of, respectively, 12.3 , 13.2 , and 14.0×10^6 G. Side bands around β are also visible. The existence of dHvA frequencies in the range of 12×10^6 G has also been reported very recently by Marker *et al.*¹⁶ from a longitudinal magnetoresistance measurement with $\vec{B} \parallel \vec{c}$. These higher frequencies have been seen by us only near the hexad axis and it is impossible to know from what parts of the FS these oscillations arise because their orientation dependence and therefore their symmetries are unknown. Figures 4 and 5 show the orientation dependence of the low-frequency dHvA oscillations in the $(10\bar{1}0)$ plane. The α frequencies which have been observed up to 84° from the hexad axis are composed of two branches. For $\vec{B} \parallel \vec{c}$ there is only one α frequency, i. e., the two α branches are degenerate for this orientation. The lower α_1^1 branch has a minimum about 3% lower than its value for $\vec{B} \parallel \vec{c}$ near 24° from the hexad axis. This minimum has also been found at the same value for negative angles. For $\vec{B} \parallel \vec{c}$, α_1^1 has a flat relative maximum at 0° . These features lead us to assume that the α frequencies correspond to what Watts¹⁷ calls type C, which may have as characteristic points in the Brillouin zone (BZ) the points M , L , S , T , R , Σ , S' , T' , and U (Fig. 6).

For our guidance we have compared the orientation dependence of these α frequencies to that of ellipsoids. Separate least-squares fits were made for the two branches, and this is the reason why

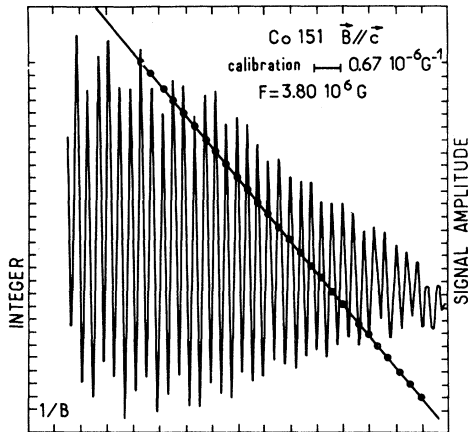


FIG. 2. Typical β dHvA oscillation. The amplitude is plotted as a function of B^{-1} , where $B = H + H_I$, with $H_I = 14700$ G is this case. One can check the B^{-1} periodicity by fitting a straight line to the B^{-1} values of the extreme positions vs integers.

the solid lines on Fig. 4, representing this ellipsoidal fit, do not intersect for $\vec{B} \parallel \vec{c}$.

For the α_1^+ branch an ellipsoidal fit is unsatisfactory because it cannot explain the simultaneous existence of a minimum at 24° and of a relative maximum at 0° . A more complex geometrical model must be used.

This oscillation near the hexad axis has the same frequency as the one observed in Shubnikov-de Haas experiments by Reed and Fawcett⁸ and attributed by them to a magnetic breakdown phenomenon.

The β oscillation has only one branch and was observed for angles comprised between -39° and $+39^\circ$. For angles $(\vec{B}, \vec{c}) > 39^\circ$, β suddenly disappears.

Following Watts,¹⁷ β would be of type A and may have as characteristic points in the BZ the points A, Γ , Δ , K, and H. The β oscillation has been measured for both positive and negative angles in order to minimize the systematic sample-misorientation errors, which may alter the analysis of the results since β varies steeply with angle. This variation of β has been least-squares fitted to the one corresponding to a quadric surface.

The fit is good, with a rms deviation of 1%. In the angular range where β was observed (-39° , 39°) the cross sections of the three types of quadric surfaces (hyperboloid, cylindrical, ellipsoid) can fit our experimental data with approximately the same rms deviation, but the feature that β disappears suddenly for $(\vec{B}, \vec{c}) > 39^\circ$ means that the surface opens for higher angles and suggests a hyperbolic neck.

From day to day one finds fluctuations of the order of 5% in the frequency determination. These fluctuations may possibly result from irreproducible image effects associated with the presence of

a ferromagnetic specimen in the superconducting coil. These effects are not observed with nonferromagnetic samples.¹⁸

C. Effective Masses

The effective mass is obtained from the temperature variation of the amplitude of the dHvA oscillations $A(T)$, for a given magnetic field, after very-low-frequency filtering of the signal to get only one dHvA frequency; m^* is obtained iteratively, from Eq. (2) by a linear least-squares fit to the expression

$$\ln\left(\frac{A(T)}{T} (1 - e^{-2\alpha m^* T/B})\right) = \frac{\alpha m^* T}{B} + C, \quad (6)$$

where $\alpha = 2\pi^2 k/\hbar e$ and C is an unknown constant. The first iteration is made with the exponential factor neglected. Eight temperature points and 15 values of magnetic field were used. m^* is chosen after averaging for the different magnetic fields used. Figure 5 shows the angular variation of the effective mass for the β oscillation. m_β^* increases

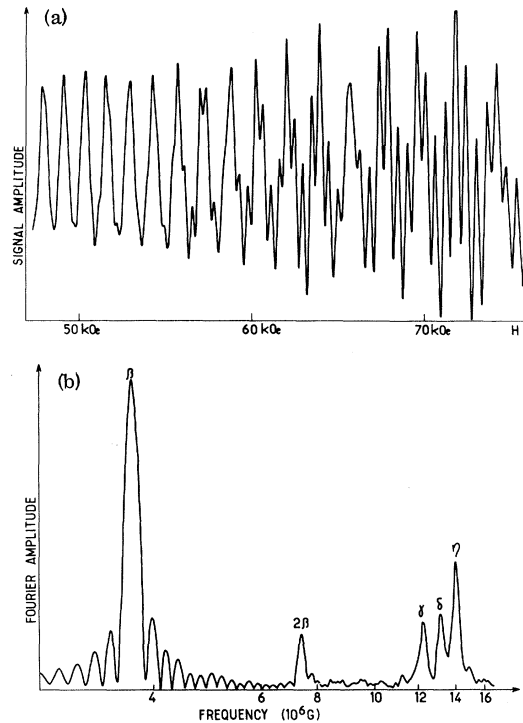


FIG. 3. (a) Typical dHvA oscillations at high magnetic field at the lowest temperatures (1.1 K), for the $\vec{B} \parallel \vec{c}$ direction, showing high-frequency oscillations. The amplitude is plotted as a function of the applied magnetic field H . The specimen is a cylinder elongated along the c axis with $H_I = 17900$ G. (b) Corresponding Fourier spectrum (the frequencies are on a logarithmic scale). The following dHvA frequencies (in 10^6 G) are visible: 3.7 (β), 7.4 (2β), 12.3 (γ), 13.2 (δ), 14.0 (η). The peaks around β are side bands originating from the limited field range used.

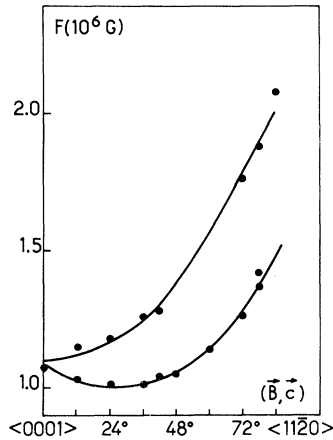


FIG. 4. Angular variation of the α frequencies in the $(10\bar{1}0)$ plane. Points correspond to experimental values and solid lines represent the least-squares fit to an ellipsoidal surface made separately for the two branches. For $\vec{B} \parallel \vec{c}$ there is only one α frequency.

as the β frequency increases. The error on m_β^* is estimated to be about 15%. The minimum value for m^* is

$$m_\beta^*(0001) = (0.20 \pm 0.03)m_0.$$

The effective mass for the α oscillation has been obtained earlier³ for the \vec{c} hexad axis parallel to \vec{B} . We have

$$m_\alpha^*(0001) = 0.08 m_0.$$

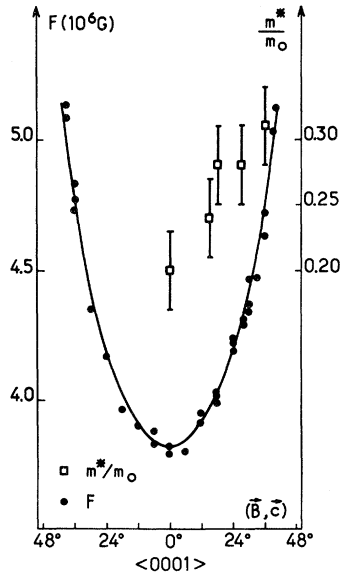


FIG. 5. Angular variation of the β dHvA frequency and the corresponding effective mass. The β oscillation disappears for (\vec{B}, \vec{c}) angles larger than 39° . The solid line represents the least-squares fit to a hyperbolic neck.

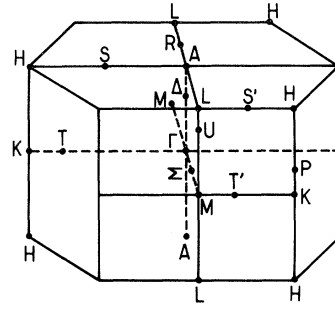


FIG. 6. First BZ for the hcp cobalt. The ΓA , ΓM , and ΓK directions correspond, respectively, to the $[0001]$, $[10\bar{1}0]$, and $[11\bar{2}0]$ crystallographic directions.

IV. THEORETICAL PREDICTIONS FOR COBALT BAND STRUCTURE AND FS

Until now the band structure of cobalt is far from being well known. All the computations have been made from first principles and are generally limited to the density of states. The authors try to find agreement with results of photoemission studies and to evaluate the exchange energy. To interpret our results we will use two calculations, that of Connolly⁵ and that of Wakoh and Yamashita,⁶ referred to as I and II, respectively.

In I, Connolly applies the augmented-plane-wave (APW) method to cobalt with a local optimized spin-dependent potential. He computes the ΓALM section of the FS for spin- \uparrow (Fig. 7), which has, as far as we are concerned, the peculiarity that there is a neck at the Γ point of the BZ. This neck, in the $[0001]$ direction, corresponds to a neck in the $\langle 111 \rangle$ direction for fcc Co, as found in Cu and Ni. The spin- \uparrow bands have a similar structure to the spin- \downarrow bands, but are shifted by about 2 eV. This value seems too high.⁹

In II, Wakoh and Yamashita use the Green's-function method to compute the band structure of paramagnetic cobalt. Then, by imposing a value of $1.56 \mu_B/\text{atom}$ in a rigid-band model, they compute the spin- \uparrow and spin- \downarrow FS of ferromagnetic cobalt. They find (Fig. 8) that the spin- \uparrow Fermi level intersects $s-p$ bands and that the spin- \uparrow FS (Fig. 7) does not present a neck at the Γ point; on the other hand, the spin- \downarrow Fermi level intersects d -like bands strongly hybridized with the $s-p$ bands and the spin- \downarrow FS (Fig. 9) presents the peculiarity of the existence of a hole (or electron) pocket which is very sensitive to the crystal potential. The exchange energy is found to be 1.71 eV. This value is also too high, as compared to the one found by Eastman.⁹ Wakoh and Yamashita conclude that to reduce this discrepancy one must use a potential which lowers the $s-p$ bands with respect to the d bands. The spin- \uparrow FS will then be modified,

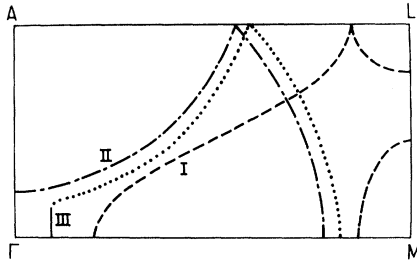


FIG. 7. Section of the spin- \uparrow FS by the Γ ALM plane of BZ according to Connolly (I) (Ref. 5), Wakoh and Yamashita (II) (Ref. 6); III is II modified by us to explain our results. Solid line corresponds to our observed values.

whereas the spin- \downarrow FS will hardly be affected.

The ratio of the experimental¹⁹ to their theoretical value of the electronic specific heat is 1.71, which implies a many-body enhancement of 0.71. But, as the theoretical value is very sensitive to the fine structure of the density of states, this enhancement value has to be viewed critically.

V. INTERPRETATION OF RESULTS

With the help of the models in I and II, we will try to interpret our experimental results. For this task dHvA frequencies may be converted to areas by the relation

$$\alpha (\text{a. u.}) = 2.673 \times 10^{-9} F (\text{G}). \quad (7)$$

A. α Frequencies

We may try to assign the α frequencies to a pocket in the spin- \downarrow FS located at the U point of the BZ (Fig. 9) since such a pocket was found in II.

In this case the α frequencies would arise from 12 half-pockets with 10^{-4} electrons/atom for each

pocket. This pocket, contrary to II, is elongated in the LM direction.

This interpretation has to be taken cautiously because of the existence of a minimum at 24° from the hexad axis for the α_1^{\downarrow} branch. It is possible that this anomalous angular variation is related to some combined action of spin-orbit and exchange interactions as found for the d -hole pocket in Ni.¹⁸ It has to be mentioned that the pocket at the U point found in II is very sensitive to the potential as to its shape, dimensions, and exact position in the BZ. Also, the choice of the potential in II is questionable because the position of the s - p bands relative to the d bands is poorly defined, and above all the treatment of the exchange interaction is unsatisfactory since the exchange splitting is introduced at the end of the computation by imposing the Bohr magneton number. Consequently, the fine-structure details of the FS predicted by II have to be taken with caution.

B. β Frequencies

The β oscillations may be assigned to the existence of a neck at the Γ point of the spin- \uparrow FS. As may be seen from Figs. 7 and 8, the condition for the existence of a neck is

$$E_{F\uparrow} > E_{\Gamma\uparrow}. \quad (8)$$

From the β dHvA frequency one finds a cross section $\alpha_\beta(0001) = 9.73 \times 10^{-3}$ a.u. Then, assuming a circular cross section for the neck, the radius will be $k_\beta = 0.056$ a.u.

In I Connolly finds for the spin- \uparrow FS a neck at the Γ point with a dimension 0.12 a.u. This implies a cross section about four times larger than we have found. However, in I the exchange energy is approximately 2 eV. This value of exchange is too

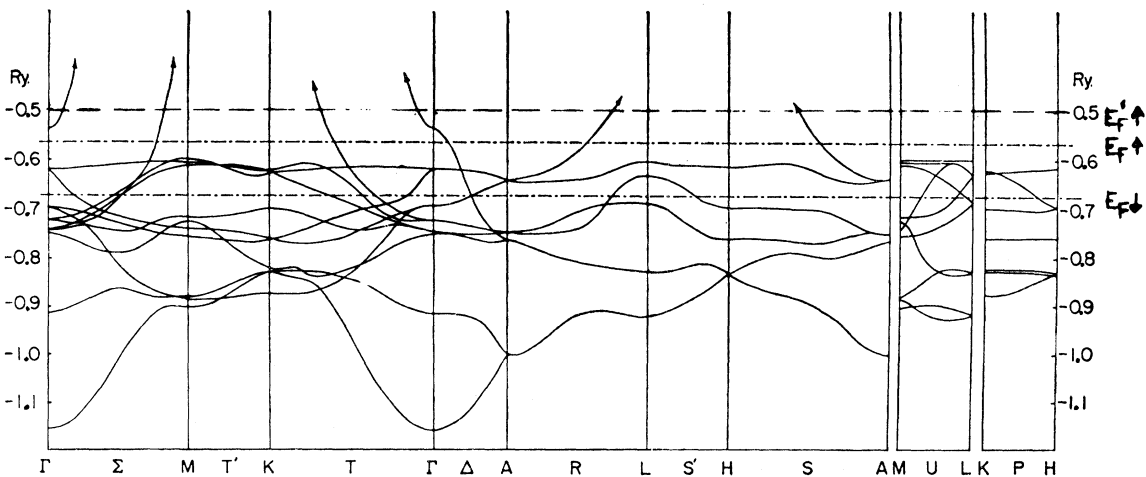


FIG. 8. Band structure of hcp cobalt proposed by Wakoh and Yamashita (Ref. 6) showing the spin- \uparrow ($E_{F\uparrow}$) and spin- \downarrow ($E_{F\downarrow}$) Fermi levels and the spin- \uparrow ($E_{\Gamma\uparrow}$) Fermi level shifted by us, which may account for our results.

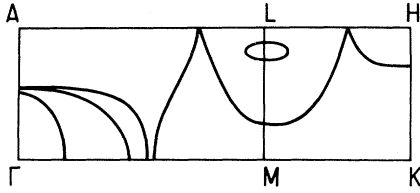


FIG. 9. Section of the spin- \uparrow FS by the Γ ALM and LMKH planes of BZ according to Wakoh and Yamashita (Ref. 6) showing an ellipsoidal pocket with U symmetry.

large, but agrees with the number of Bohr magnetons/atom. If we shift the spin- \uparrow Fermi level to reduce the exchange splitting, the shift works in the proper direction to give our neck dimensions.

In II (Fig. 9) we see that $E_{F\uparrow} < E_{\Gamma_3^+}$, so that there is no neck at Γ , but the exchange energy $\Delta E = 1.71$ eV calculated by Wakoh and Yamashita is also too large as compared to the 1.05 eV found experimentally by Eastman.⁹ As Co is a strong⁴ ferromagnetic metal, the spin- \uparrow bands have a s - p character. Instead of taking a new potential which would shift the s - p bands down relative to the d bands, for the spin- \uparrow FS we may take advantage of the fact that Co is a strong ferromagnetic metal. Then using a rigid-band model one may produce qualitatively the same effect by shifting up the spin- \uparrow Fermi level by the same amount.

For a hyperbolic neck the energy relative to the $E_{\Gamma_3^+}$ energy can be expressed by

$$E_{\text{neck}} = E_{F\uparrow} - E_{\Gamma_3^+} = \frac{\hbar^2}{2} \left(\frac{k_{\perp}^2}{m_{\perp}} - \frac{k_{\parallel}^2}{m_{\parallel}} \right), \quad (9)$$

where k_{\parallel} , m_{\parallel} and k_{\perp} , m_{\perp} are the coordinates and band masses longitudinal and transverse to the hexagonal axis (relative to the Γ point).

In particular, for $\vec{E} \parallel \vec{c}$ we may write

$$E_{\text{neck}} = \frac{\hbar^2}{2\pi} \frac{\alpha_{\beta}(0001)}{m_{\perp}}. \quad (10)$$

The β -effective mass found along the hexad axis is (Fig. 5)

$$m_{\beta}^*(0001) = (0.20 \pm 0.03)m_0.$$

This mass, which includes many-body effects, is linked to the transverse-band mass by the relation

$$m_{\beta}^*(0001) = m_{\perp} (1 + \lambda),$$

where λ is the enhancement by many-body effects,

mainly electron-phonon and electron-magnon interaction. Information about λ in Co is lacking, but Phillips²⁰ has estimated λ to be 1.8 for Ni. If we take values from 0 to 2 for λ , we find values from 0.017 to 0.051 Ry for E_{neck} .

In II, $E_{\Gamma_3^+} - E_{F\uparrow} = 0.014$ Ry, so that the shift of $E_{F\uparrow}$ in the rigid-band model will be between 0.031 and 0.065 Ry, i.e., 0.41 and 0.83 eV, which results in an exchange energy between 0.88 and 1.30 eV in excellent agreement with Eastman's experimental result⁹ and Wohlfarth's estimation.⁴ The value 1.05 eV is found with a many-body mass enhancement of 1.

VI. CONCLUSION

We have used the low-frequency field-modulation method to investigate the dHvA effect in cobalt in the $(10\bar{1}0)$ plane.

Two types of oscillations are presented, α and β . The α frequencies $[(1-2) \times 10^6 \text{ G}]$ have two branches and, in agreement with the Wakoh and Yamashita calculations,⁶ may be tentatively assigned to a pocket of U symmetry in the spin- \uparrow FS. Since the α oscillation is very sensitive to the crystal potential, it may be a very useful test for the fine structure of the band calculations, and, in particular, for interpolation schemes.

The β frequencies $[(3-5) \times 10^6 \text{ G}]$ have one branch and are observed up to 39° away from the hexad axis. Their angular variation corresponds to a hyperbolic neck at the Γ point. This neck is found in the spin- \uparrow FS if some modifications are made in the published models of FS,^{5,6} mainly the reduction of exchange energy to 1.05 eV, in agreement with recent⁹ photoemission conclusions. The hyperbolic β neck may be useful to evaluate the many-body mass enhancement and to fix the $E_{\Gamma_3^+} - E_{F\uparrow}$ energy and can help to find the shift between the s - p bands and the d bands.

We are now investigating the high-frequency oscillations γ , δ , and η (Fig. 3) and the possibility of magnetic breakdown of the α oscillation and its connection to the magnetoresistance.

ACKNOWLEDGMENTS

We are grateful to Professor J. Friedel for directing our attention to this subject and for comments during this work. We wish to thank Miss R. M. Meunier and R. Leleu for technical assistance.

¹C. Herring, *Magnetism* (Academic, New York, 1966), Vol. IV.

²A. V. Gold, in *Solid State Physics* (Gordon and Breach, New York, 1968), p. 39.

³F. Batallan and I. Rosenman, in *Proceedings of the Twelfth International Conference on Low Temperature Physics, Kyoto, 1970*, edited by Eizo Kanda (Keigaku,

Tokyo, 1971), p. 595.

⁴E. P. Wohlfarth, *J. Appl. Phys.* **41**, 1205 (1970).

⁵J. D. Connolly, *Intern. J. Quantum Chem.* **11S**, 257 (1968).

⁶S. Wakoh and J. Yamashita, *J. Phys. Soc. Japan* **28**, 1151 (1970).

⁷L. Hodges and H. Ehrenreich, *Phys. Letters* **16**, 203 (1965); F. M. Mueller, *Phys. Rev.* **153**, 659 (1967).

⁸W. Reed and E. Fawcett, *Proceedings of the Nottingham Conference on Magnetism* (Inst. Phys. and Phys. Soc., London, 1964), p. 120.

⁹D. E. Eastman, *J. Appl. Phys.* **40**, 1386 (1969).

¹⁰D. Schoenberg and P. J. Stiles, *Phys. Letters* **4**, 274 (1963).

¹¹R. W. Stark, *Phys. Rev.* **162**, 589 (1967).

¹²The line frequency is 50 cps.

¹³J. R. Anderson and A. V. Gold, *Phys. Rev. Letters* **10**, 227 (1963).

¹⁴R. W. Stark and D. C. Tsui, *J. Appl. Phys.* **39**, 1056 (1968).

¹⁵The influence of the anisotropy energy on the data can be fairly well neglected as may be shown. When \vec{H} is not parallel to the easy magnetization direction, i. e., the \vec{c} axis, the resultant magnetic induction \vec{B} may not be parallel to \vec{H} . A simple calculation taking into account the anisotropy energy and the magnetic energy of the sample shows that this occurs only for fields H smaller than H_0 . For the most difficult magnetization direction, i. e., perpendicular to the \vec{c} axis, we find that $H_0 = (2K_1 + 4K_2)/M_s$

if the specimen is saturated. K_1 and K_2 are the anisotropy constants for cobalt at 4.2°K. With adequate values for the parameters [see, for example, R. Pauthenet, Y. Barnier, and G. Rimet, *J. Phys. Soc. Japan Suppl. B-I* **17**, 309 (1962)] one finds $H_0 \approx 14$ kOe. We may neglect the effects of the anisotropy energy because we are working in a range of magnetic fields (>30 kOe) sufficient to saturate the specimen (see R. Pauthenet *et al.*), and fairly far above H_0 (the field necessary to align the magnetization, and hence \vec{B} , with \vec{H}).

¹⁶D. L. Marker, J. W. Reichardt, and R. V. Coleman, *J. Appl. Phys.* **42**, 1338 (1971).

¹⁷B. R. Watts, *Proc. Roy. Soc. (London)* **A282**, 521 (1963).

¹⁸L. Hodges, D. R. Stone, and A. V. Gold, *Phys. Rev. Letters* **19**, 655 (1967).

¹⁹C. H. Cheng, C. T. Wei, and P. A. Beck, *Phys. Rev.* **120**, 426 (1960).

²⁰J. C. Phillips, in *Proceedings of the International School of Physics "Enrico Fermi," Course XXXVII*, edited by W. Marshall (Academic, New York, 1967).

Theory of the Inelastic Scattering of Low-Energy Electrons from Crystal Surfaces by One-Phonon Processes*

V. Roundy and D. L. Mills†

Department of Physics, University of California, Irvine, California

(Received 21 May 1971)

In this paper, we present a theoretical discussion of the form of the differential cross section per unit solid angle per unit energy shift for the inelastic scattering by one-phonon processes of low-energy electrons from the surface of a semi-infinite crystal. A number of general features of the cross section are discussed, with particular attention to a comparison with the results obtained from the kinematical theory of the scattering process. We have also carried out a series of numerical studies of the dependence of the shape of the energy-loss spectrum on momentum transfer for an electron incident on the (100) surface of a model fcc crystal. For a general value of the momentum transfer, the energy-loss spectrum consists of one or more lines that arise from the scattering off surface modes, and a band that has its origin in scattering produced by bulk modes. The shape of the latter feature, as well as the position of the surface-mode peaks, is found to be quite sensitive to the values of the atomic force constants appropriate to the surface layer. It is suggested that the experimental study of the shape of the loss spectrum will provide a powerful means of probing the frequency spectrum of the atomic vibrations near the surface.

I. INTRODUCTION

In recent years, a considerable amount of effort has been devoted to the study of the vibrational amplitudes of atoms in crystal surfaces. A number of theoretical approaches to the problem have been developed.¹ Experimentally, one may infer the amplitude of the mean-square displacement in the surface from the temperature dependence of the intensity associated with the elastic scattering of low-energy electrons from the surface. If one utilizes a kinematical description of the scattering process, then the temperature dependence of the

low-energy-electron diffraction (LEED) intensity has its origin in the Debye-Waller factors that appear in the expression for the cross section.² When the Debye-Waller factors are extracted from the data, one may obtain information about the magnitude of the mean-square displacement in the surface, as well as the anisotropy that results from the lowered site symmetry in the surface layer. Most analyses carried out by this method assume the validity of the kinematical theory. Laramore and Duke³ have recently completed a detailed analysis of the temperature dependence of the LEED intensity; we refer the reader to their